Three Phase Indirect Matrix Converter Act as a DC/DC Boost Converter

Manthri Sravanthi
P.G. scholar, Dept of EEE
VVIT,Chevella

Rajesh Thipparapu
P.G. scholar, Dept of EEE
SCCEngg Karimnagar

G.Sridhar Babu
HOD, Dept of EEE
VVIT, Chevella

Abstract—**An indirect matrix converter (IMC) connected with two input power sources is proposed: a gasoline generator as the main ac power supply and batteries as the secondary power source. The IMC is small in size because of having a dc-link part without an electrolytic capacitor. The dc-link part is utilized by connection with a boost-up chopper with batteries as a secondary input power source. Furthermore, the chopper connects to the neutral point of the motor and utilizes the leakage inductance of the motor as a reactor component. The proposed technique successfully further reduce the size of the converter by removing the boost reactor in the boost converter stage. The proposed converter is simulated The total harmonic distortion of the input and output currents are 4% and 3.7%, respectively, and the efficiency is 96%.**

Index Terms—**Boost-up chopper, leakage inductance, neutral point of a motor, three-phase ac/ac converter, zero-vector switching.**

I.   INTRODUCTION

ENVIRONMENTAL responsibility has become a significant concern for communities so that the development of renewable power sources, such as wind turbines and low-carbon-emission hybrid electric vehicles (HEVs) is progressing rapidly. One of the most common applied converters in hybrid systems is the ac/dc/ac converter because it has the ability of connecting to two different power sources. The generator mainly supplies constant power to the load and a battery is used as an alternate power source to drive an electric motor and also to absorb the power fluctuation during periods of high peak energy demand. Fig. 1 shows a conventional ac/dc/ac power converter, which typically consists of a pulse width modulation (PWM) rectifier, a dc-link capacitor, and a PWM inverter, also known as a back to-back (BTB) system [1]–[3]. The PWM rectifier is often used to reduce the harmonic currents in a generator and control the dc-link voltage [2], [4]–[6]. In order to obtain high performance under an adjustable speed drive system, a constant dc-link voltage is required in a BTB system because the voltage fluctuation of the dc-link part will cause an output voltage error. A typical method for reduction of the voltage fluctuation is to place a large electrolytic capacitor into the dc-link part as a filtering device between the rectifier and the inverter. However, a large electrolytic capacitor is bulky.

Another approach is to reduce the capacity of the electrolytic capacitor by the application of a high-speed dc-voltage controller to the rectifier control [7]. However, the control response is limited by the delay of the voltage detection and digital controller; therefore, the electrolytic capacitor is still required. In addition, the capacitance is not reduced, since the dc-link capacitor is dominated by the capacitor
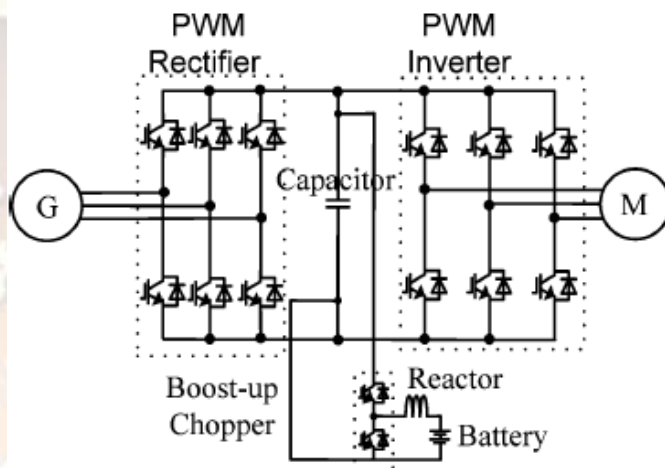

Fig. 1. Back-to-back converter.

current. As a result, a large amount of space is required for the capacitor installation in a practical device. In addition, electrolytic capacitors are not suitable for high-temperature applications, such as in HEVs Overall, these disadvantages of the electrolytic capacitor affect the reliability of the converter.

For the secondary input power source, a boost converter that consists of a boost reactor and a switching leg [insulated gate bipolar transistor (IGBT)] is connected with batteries to the dc link part of the BTB system. Boost converter will control the battery current and the battery power will be used as a secondary power to drive the electric motor.

In this paper, a new circuit topology is presented, which is composed of an indirect matrix converter (IMC) and a dc/dc boost converter that connects to the neutral point of a motor. An IMC has high efficiency and is easily configured in comparison to matrix converters [8]–[12]. In addition, this converter does not require a dc-link electrolytic capacitor to filter the dc-ripple voltage. It uses a direct conversion technique where the frequency of the dc-link voltage contains a ripple with six times of the input frequency. However, the output voltage transfer ratio is limited by this direct conversion technique which is

similar to the matrix converter, where output voltage = 0.866 of the input voltage [13].
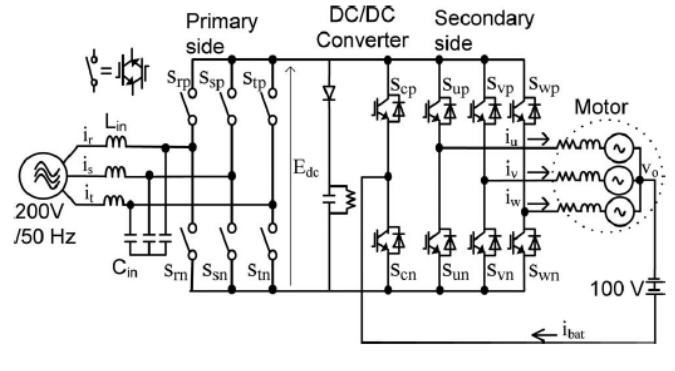

Fig. 2. Proposed circuit topology.

Nevertheless, an appropriate control over the inverter is also proposed so that it is possible to connect a dc chopper to the neutral point of the motor and to operate as a dc/dc converter [14]. This dc/dc converter with a battery is performed as a secondary power source of the IMC to drive the electric motor. The proposed circuit utilizes the neutral point of a motor in the boost converter because the leakage inductance of the motor can be used as a reactor. Generally, the leakage inductance is around 10% of the rating impedance in an induction motor. For the proposed dc converter, around 3% of the reactor is enough to use as a boost reactor component. Please note that the synchronous reactance in a permanent motor is higher than the leakage inductance of an induction motor.

By removing the electrolytic capacitor and the boost-up reactor, the remaining part of the proposed circuit is constructed only of silicon components, namely, IGBTs and diodes. As a result, the proposed circuit is highly efficient and highly reliable. Simulation and experimental results clearly demonstrate that the circuit is capable of providing sinusoidal waveforms for the input and output, and high efficiency and a high power factor can be achieved.

II.   PROPOSED CIRCUIT TOPOLOGY

Fig. 2 shows the proposed circuit configuration. The IMC can be simply divided into primary and secondary stages. The primary stage for the ac power source consists of 12 units of reverse-blocking IGBTs [15], also known as a current-source rectifier ,where bidirectional power flow is possible in this circuit structure. A *LC* filter is required at the input of the primary stage to smooth the input current. The secondary stage for the motor consists of six IGB Tunits ,which is similar to a standard voltage source inverter. The advantage of this converter over a BTB is that the primary side does not contain switching loss because zero-current switching can be applied. The switching timing of the primary side is during the zero-current period of the dc-link when the secondary stage output zero voltage. Therefore, high efficiency is achievable in this converter [11].

The other reason to use the IMC is that the IMC has a dc-link part, which is different than the conventional matrix converter. The dc-link part is utilized by adding a boost converter to the IMC. The boost converter connects to the battery and the other terminal of the battery is then connected to the neutral point of the motor.

A snubber circuit is also included in the dc-link part to absorb the voltage overshoot from reactive elements in the circuit [16].It is used to prevent damage to the switching devices in the secondary side due to a sudden large voltage. It should be noted that the capacity of the snubber capacitor is smaller than the dc-link capacitor in a BTB system, because the ripple current of the dc-link part does not flow in

the snubber capacitor. The chopper circuit is connected in the dc link and batteries are connected to the neutral point of the motor. The leakage inductance of the motor is used as a boost-up reactor in the proposed circuit. As a result, the proposed converter does not require bulky passive components.

III.   CONTROL STRATEGY

Fig. 3(a) shows a control block diagram of the proposed circuit. The primary side, the dc chopper, and the secondary side are individually controlled by their own commands. A carrier comparison method is used as the PWM modulation, according to the control strategy [17]. The relationship between the output and input voltages is obtained by (1). The secondary side operates as a four-phase voltage-source inverter by addition of the dc chopper as the fourth leg

$$\begin{bmatrix} v_u \\ v_v \\ v_w \\ v_{bat} \end{bmatrix} = \begin{bmatrix} S_{up} & S_{un} \\ S_{vp} & S_{vn} \\ S_{wp} & S_{wn} \\ S_{cp} & S_{cn} \end{bmatrix} \begin{bmatrix} S_{rp} & S_{sp} & S_{tp} \\ S_{rn} & S_{sn} & S_{tn} \end{bmatrix} \begin{bmatrix} v_r \\ v_s \\ v_t \end{bmatrix} \quad (1)$$

where S_{xy} represents the switching function of the switches. When sxy is turned ON, $S_{xy} = 1$, and when S_{xy} is turned OFF, $S_{xy} = 0$.
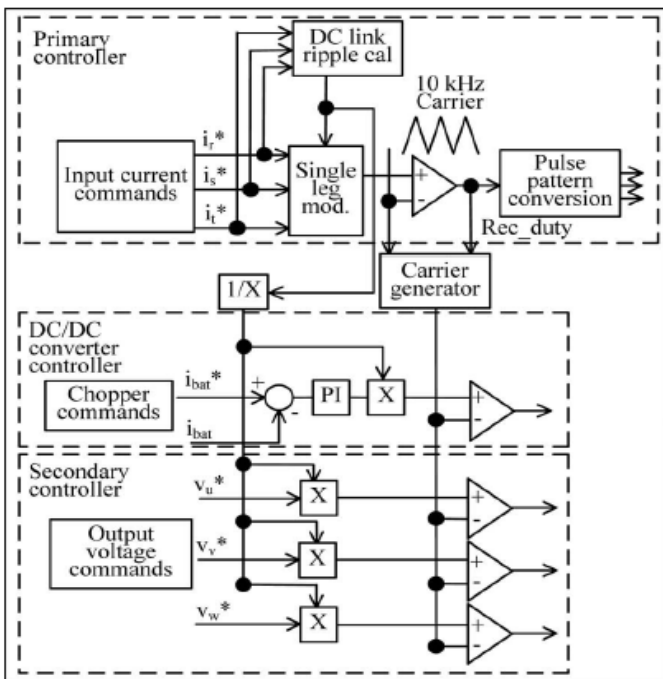
A.   Primary-Side Control

The primary-side controller is designed with a current-type PWM rectifier command. It uses a pulse-pattern conversion to convert the PWM pulses of the voltage source type into the PWM pulse of the current source type by a simple logic selector. It uses a single-leg modulation where the switching period can be reduced from $2\Pi/3$ to $\Pi/3$, where the $2\Pi/3$ is the switching period of the conventional two-phase modulation [15]. That is, the leg with the maximum input phase voltage will always be turned ON, and the other two legs will be always turned OFF, as shown in Fig. 3(b). When the maximum input phase voltage is changing, (for example, from $+R$-phase to $-S$-phase), the related max phase voltage leg and the mid phase voltage leg will be switched at zero current until the relevant

switch that contains the mid phase voltage becomes the maximum input phase voltage. From this direct conversion technique, a dc-link voltage that contains a ripple with six times of the input frequency will be formed

B. Secondary-Side Control

A conventional controller method for a voltage-source-type inverter is applied to the dc chopper and the inverter with a lean controlled carrier modulation. The carrier modulation forms a new carrier, where the peak position of the triangular carrier is controlled by the duty ratio of the rectifier-side pulse. This rectifier pulse is used to control the switching timing of the primary stage and the zero-vector of the secondary stage. From the control, zero-current switching is achieved in the primary stage, where the dc-link current becomes zero at the peak of every carrier. This new carrier is then used in the secondary side and the dc chopper side as a normal PWM comparison method, also referred to as an inverter carrier. The boost converter is not a stand-alone circuit in the proposed circuit. Operation is strongly dependent on the secondary side of the IMC. Zero-vector outputs on the secondary side are the key factor to link the boost converter to the IMC. The zero vector controls the amplitude of the output voltage. There are two functions of the zero-vector output to the secondary side. The first is to implement zero-current switching on the primary side so that the switching losses do not occur at the primary side. The second function involves operation of the boost converter, which will be described in a later chapter.

applied to the secondary side. The inverter commands are given by the voltage controller as described in Chapter IV. It is noted that the dc chopper is controlled as the fourth leg of the inverter so that the dc chopper command is compared by the same carrier with the inverter voltage commands. There are two methods to generate an inverter carrier; Fig. 4(a) represents the symmetrical type, which has approximately double the switching frequency of the rectifier switching frequency, and Fig. 4(b) shows the asymmetrical type, which has the same switching frequency as the rectifier switching frequency [16].

In Fig. 4(a), the bottom peak position of the triangular carrier is controlled by the duty ratio of the rectifier pulse, as shown in the upper part of the figure. The chopper commands, along with the inverter output voltage commands, are compared with this new inverter carrier to obtain the desired switching patterns. The zero-vector periods are shown in the lower part of Fig. 4(a). The switching pulses of the secondary side attain the zero vectors for every carrier cycle. The primary side arms switch at every zero-vector period.

In Fig. 4, zv_u and zv_l represent the zero-vector periods of the inverter, where $zv\ u = Sup = Svp = Swp = 1$ (upper arm zero vector) and $zv\ l = Sup = Svp = Swp = 0$[lower arm zero vector $(Sun = Svn = Swn = 1)$]. The upper arm of the chopper (Scp) switches ON at every zero-vector period of zv_u. On the other hand, the lower arm of the chopper (Scn) will switch ON at every zero-vector periods of zv_l. During these zero-vector periods, the boost converter is operated in the ON-state, and the battery current through the leakage inductance of the motor increases. During the nonzero-vector periods, also known as the OFF-state operation, the battery current is released into

(a)Fig. 3 (a) Control block diagram. (b) Primary-side-switching pattern.
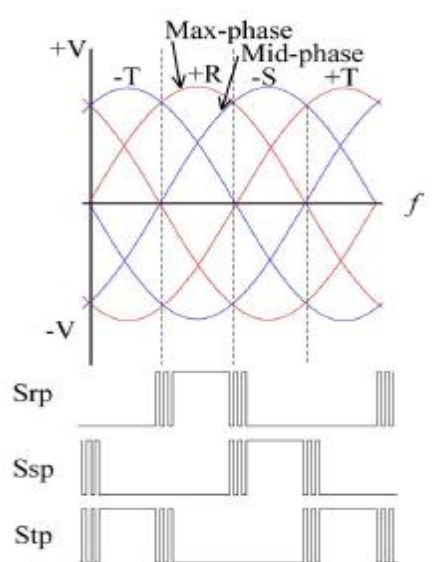
(b)

Fig. 4 shows an example of the relationship between the normal carrier applied to the primary side and the new inverter carrier

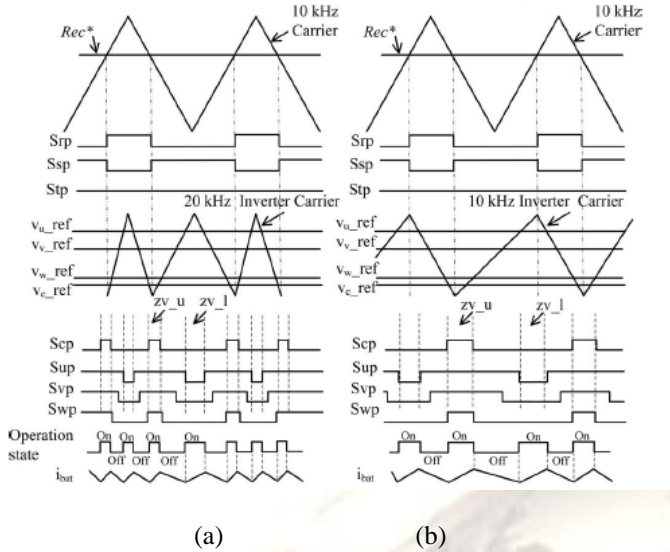(a)   (b)

Fig. 4. Relationship between the zero vectors and boost converter operation. (a) Symmetrical inverter carrier. (b) Asymmetrical inverter carrier

the capacitor in the *LC* filter at the power source. The operation state in the figure is referred to the boost converter operation.

When the switching frequency of the rectifier is 10 kHz, the control method applied in Fig. 4(a) generates a new symmetrical carrier that has a frequency of approximately 20 kHz. This is approximately twice the primary-side switching frequency. Alternatively, according to Fig. 4(b), an inverter carrier can be formed based on the duty of the rectifier command, which is asymmetrical with a frequency of 10 kHz.

By comparing the symmetrical and asymmetrical inverter carriers in Fig. 4, it should be noted that the zero-current switching in the rectifier is not affected by the inverter carrier because both carriers are formed following the rectifier duty. Since every carrier time is longer in the asymmetrical inverter carrier, the sequence of the zero-vector periods becomes slower; therefore, the boost converter will achieve better efficiency, but the current ripple in the battery will be increased. Further, the asymmetrical method can achieve better total harmonic distortion (THD) values for the output because the dead time effect is smaller due to the lower switching frequency. The other disadvantage of the asymmetrical inverter carrier is the detection of the load current. Usually, the average value of the load current appears at the peak of the symmetrical inverter carrier so that it can be easily detected using the symmetrical inverter carrier. However, for the asymmetrical carrier, the average current point does not agree with the peak of the asymmetrical carrier; therefore, in order to detect the average current, a lowpass filter is required. Consequently, control performance will be decreased

IV. UTILIZATION OF THE NEUTRAL POINT OF THE MOTOR

The voltage commands of the secondary stage are decided by the battery current command and the output voltage commands for the three-phase load. A three-phase inverter has eight output voltage space vectors, including two zero vectors. The importance of the zero vectors explains the behavior of the boost converter along with the neutral point of the motor. The boost converter will operate at every zero vector of the secondary side of the converter. On the other hand, the output voltage for the three-phase load is controlled by other voltage vectors, as shown in [14].

Fig. 5 illustrates the output current-flow diagram of the secondary side under the normal operation and Fig. 6 shows the zero-phase-sequence equivalent circuit, where the battery is operating at discharge mode. In Fig. 5, the secondary side functions as a conventional three-phase inverter with a motor; it controls the motor speed and torque. Zero-phase sequence is happening at every zero-vector periods of the secondary side. The current at the neutral point of the motor is zero and a positive or negative battery current can be controlled, as shown in Fig. 6. Note that the polarity of the battery voltage can be connected in facing the neutral point of the motor or in a reverse way [14]. *C*in represents the capacitors from the *LC* filter; since two switches in the primary side will always be turned ON, the capacitors *C*in can be considered in the dc-link voltage. On the other hand, for the zero-phase sequence, the motor line voltage can be considered as zero so that the motor can be considered as a leakage inductance. In addition, the secondary side of the converter can be considered as a single-leg topology. The battery current first goes into the secondary side and flows out through the neutral line and charges or discharges the battery. The battery current can be controlled by the proportional–integral (PI) controller

The zero vectors are two particular vectors that generate zero line voltage to the motor. The neutral-point voltage $v0$ of the motor, based on the neutral point of the dc-link part, is obtained by the following equation:

$$\begin{cases} v_o = \frac{E_{dc}}{2} \ when \ all \ the \ upper \ arms \ are \ on \\ v_o = \frac{-E_{dc}}{2} \ when \ all \ the \ lower \ arms \ are \ on \end{cases} \qquad (2)$$

where Edc is the dc-link voltage and $v0$ is the voltage of the neutral point of the motor, based on the neutral point of the dc-link part.

A high dc-link voltage is mandatory in order to control the zero vectors; therefore, the relationship between the dc-link voltage (Edc), the inverter line voltage ($v$inv), and the battery voltage (Vbat) will be discussed. The inverter output voltage, vu , vv , and vw , with respect to the neutral point voltage of the dc link, is expressed as

Fig. 5. Secondary-side current flow diagram (normal operation).

$$\begin{cases} v_u = a\frac{E_{dc}}{2}\sin(wt) + v_o \\ v_v = a\frac{E_{dc}}{2}\sin\left(wt - \frac{2\Pi}{3}\right) + v_o \\ v_w = a\frac{E_{dc}}{2}\sin\left(wt - \frac{4\Pi}{3}\right) + v_o \end{cases} \quad (3)$$

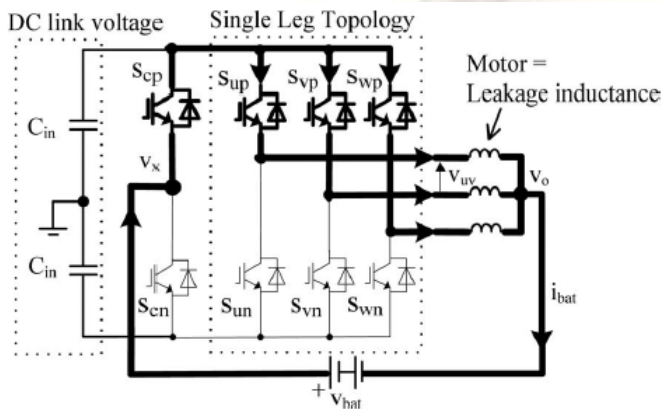Fig. 6. Zero-phase-sequence equivalent circuit.

Table 1
Simulation Parameters

Input voltage	200 V	DC source	100 V
Input frequency	50 Hz	Output voltage	173 V
Carrier frequency	10 kHz	Output frequency	35 Hz
Inverter frequency	10 kHz	Leakage inductance	5 mH

where a is the modulation index of the motor phase voltage, 0 $<a<$ 1, $v0$ is the neutral point voltage of the motor (during zero phase sequence), and ω is the inverter output angular frequency.The inverter line voltage is then given by ($u–v$ phase)

$$v_{uv} = a\frac{\sqrt{3}}{2}E_{dc}\sin\left(wt + \frac{\Pi}{6}\right) \quad (4)$$

Equation (5) shows the relationship for an inverter to obtain the maximum output line voltage Vinv (rms) under the maximum reference magnitude of a three-phase modulation

$$E_{dc} \geq 2\frac{\sqrt{2}}{\sqrt{3}}V_{inv} \quad (5)$$

The maximum line voltage between the inverter leg and chopper leg can be obtained as (rms)

$$v_{ux} = \frac{\sqrt{2}}{\sqrt{3}}V_{inv} + V_{bat} \quad (6)$$

Since vux must be smaller than Edc, the inverter voltage and battery voltage are constrained by the following equation

$$E_{dc} > 2\frac{\sqrt{2}}{\sqrt{3}}V_{inv} + V_{bat} \quad (7)$$

As a result, the dc-link voltage of the proposed circuit must satisfy both requirements as shown by the following equation, which can be referring to Fig. 6:

$$E_{dc} \geq \begin{cases} 2\frac{\sqrt{2}}{\sqrt{3}}V_{inv} & \text{when } \frac{\sqrt{2}V_{inv}}{\sqrt{3}} > V_{inv} \\ \frac{\sqrt{2}}{\sqrt{3}}V_{inv} + V_{bat} & \text{when } \frac{\sqrt{2}V_{inv}}{\sqrt{3}} < V_{inv} \end{cases} \quad (8)$$

Note that in (8), the Vbat can always be neutralized with half of the$E$dc under the two conditions. That is, Vbat must be always smaller than half of the Edc, since the Edc is always known as the 0.866 of the input phase voltage, as shown in the following equation:

$$\frac{\sqrt{2}}{2}V_{in}0.866 > V_{bat} \quad (9)$$

Furthermore, a new expression of the secondary-side current is given as follows, assuming that the leakage impedance is even during the zero-phase-sequence equivalent circuit

$$\begin{cases} i_u = i_a + \frac{i_{bat}}{3} \\ i_v = i_b + \frac{i_{bat}}{3} \\ i_w = i_c + \frac{i_{bat}}{3} \end{cases} \quad (10)$$

where i_u, i_v, and i_w are the inverter currents, i_a, i_b, and i_c are the positive-phase-inverter current, and $i$bat is the battery current.

IV. SIMULATION RESULTS

Table I shows the simulation parameters for both results. The proposed circuit was simulated under two conditions of battery discharge and charge by using a circuit simulator (PSIM, *Powersim Technologies Inc.*). An automatic current regulator (ACR) controller controls the battery current to a desired positive or negative value. An ideal battery current $i$bat is purposely adjusted at a specific time of 38 ms to confirm the proposed circuit performance. The motor model, which consists of three sets of voltage sources as back-electromotive forces and leakage inductances, is used in the simulation. The asymmetrical inverter carrier was used in the simulation.

Fig. 7 shows the battery discharge mode, with the battery current controlled from 0.5 to 2 A. The two waveforms show the input power supply voltages v_r, v_s, and v_t, the input currents i_r, i_s, and i_t, and the output line voltages (v_{uv}(LPF), v_{vw}(LPF), and v_{wu}(LPF)) through a low-pass filter, which has a cutoff frequency of 1 kHz, to observe the low-frequency components, the output currents i_u, i_v, and i_w, and the battery current $i$bat . The results show that the THD of both the input and output currents are less than 4%. It should be noted that at 20 ms, the input current magnitude decreases due to the increment of $i$bat ,

which indicates that the increase of the battery power leads to a decrease in generator power.

On the other hand, Fig. 8 shows the ACR controlling the battery current from 0.5 to −2 A. The battery is charged from a generator under this condition. The results also showed that when in the charging mode, both the input and output currents have good sinusoidal waveforms. At 20 ms, as the $i$bat decreases, the input current is forced to increase, because higher power is required to charge the battery. These two waveforms provide evidence of good power management between the generator and the battery.
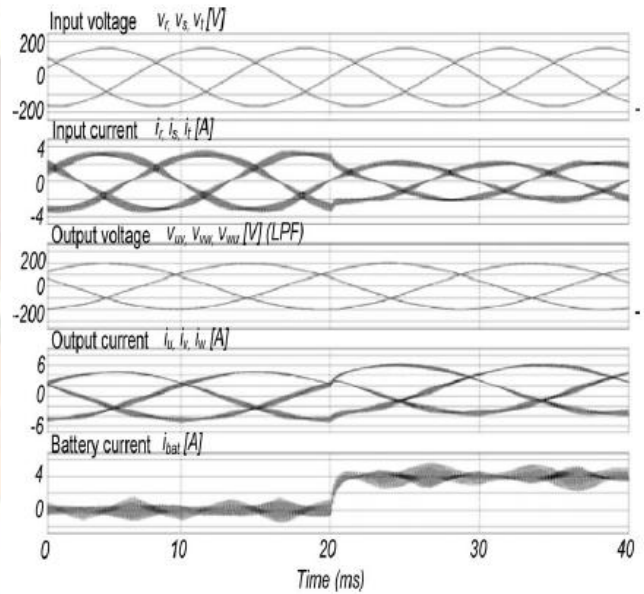

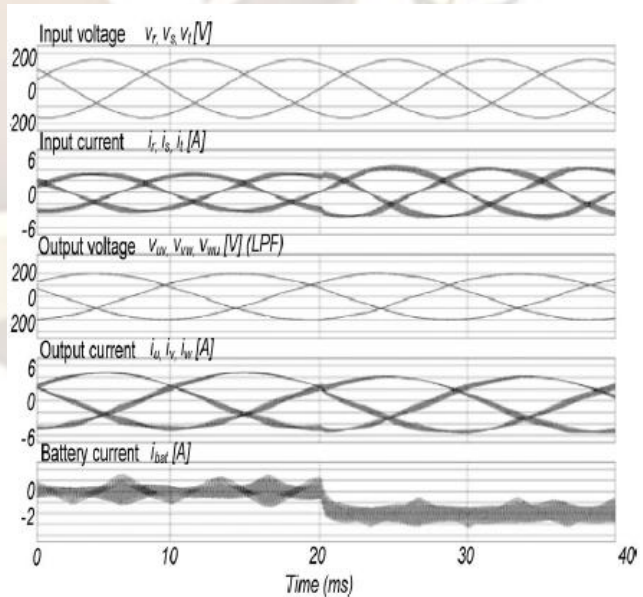Fig. 7. Simulation results (battery = discharge mode).

Fig. 8. Simulation results (battery = charge mode)

V.   CONCLUSION

A new control method is proposed by utilizing the neutral point of a motor and connection to an IMC for motor drive applications. Control over the inverter zero-vector periods allows an additional chopper leg to perform as a boost converter with connection to the neutral point of a motor. Simulation and experimental results demonstrated good sinusoidal waveforms and confirmed the validity of the proposed method. From the loss analysis of the proposed circuit, an efficiency of 96% was estimated. EMC behavior of the circuit will be subjected for further investigation.

REFERENCES

[1]   D. Casadei, G. Grandi, C. Rossi, A. Trentin, and L. Zarri, "Comparison between back-to-back and matrix converters based on thermal stress of the switches," in *Proc. IEEE Int. Symp. Ind. Electron.*, May 2004, vol. 2, pp. 1081–1086.

[2]   R. Ghosh and G. Narayanan, "Control of three-phase, four-wire PWM rectifier," *IEEE Trans. Power Electron.*, vol. 23, no. 1, pp. 96–106, Jan. 2008.

[3]   R. Lai, F. Wang, R. Burgos, Y. Pei, D. Boroyevich, B. Wang, T. A. Lipo,V. D. Immanuel, and K. J. Karimi, "A systematic topology evaluation methodology for high-density three-phase PWM AC-AC converters," *IEEE Trans. Power Electron.*, vol. 23, no. 6, pp. 2665–2680, Nov. 2008.

[4]   X. H.Wu, S. K. Panda, and J. X. Xu, "Analysis of the instantaneous power flowfor three-phasePWMboost rectifier under unbalanced supply voltage conditions," *IEEE Trans. Power Electron.*, vol. 23, no. 4, pp. 1679–1691, Jul. 2008.

[5]   B. Yin, R. Oruganti, S. K. Panda, and A. K. S. Bhat, "A simple singleinput- single-output (SISO) model for a three-phasePWMrectifier," *IEEE Trans. Power Electron.*, vol. 24, no. 3, pp. 620–631, Mar. 2009.

[6]   H.Yoo, J.-H.Kim, and S.-K. Sul, "Sensorless operation of aPWMrectifier for a distributed generation," *IEEE Trans. Power Electron.*, vol. 22, no. 3, pp. 1014–1018, May 2007.

[7]   Y. Chen and X. Jin, "Modeling and control of three-phase voltage source PWM rectifier," in *Proc. IEEE Power Electron. Motion Control Conf.*, Shanghai, Aug. 2006, vol. 3, pp. 1–4.

[8]   R.Vargas, U. Ammann, and J. Rodriguez, "Predictive approach to increase efficiency and reduce switching losses onmatrix converters," *IEEE Trans.Power Electron.*, vol. 24, no. 4, pp. 894–902, Apr. 2009.

[9]   M. Jussila and H. Tuusa, "Comparison of simple control strategies of space-vector modulated indirect matrix converter under distorted supply voltage," *IEEE Trans. Power Electron.*, vol. 22, no. 1, pp. 139–148, Jan. 2007.

[10]   T. Friedli, M. L. Heldwein, F. Giezendanner, and J. W. Kolar, "A high efficiency indirect matrix converter utilizing RB-IGBTs," in *Proc. 37th IEEE Power Electron. Spec. Conf.*, Jeju, Jun. 2006, pp. 1–7.

[11]   J.W. Kolar, F. Schafmeister, S. D. Round, and H. Ertl, "Novel three-phase AC–AC sparse matrix converters," *IEEE Trans. Power Electron.*, vol. 22, no. 5, pp. 1649–1661, Sep. 2007.

[12]   J.-I. Itoh and K.-I. Nagayoshi, "A new bidirectional switch with regenerative snubber to realize a simple series connection for matrix converters," *IEEE Trans. Power Electron.*, vol. 24, no. 3, pp. 822–829, Mar. 2009.

[13]   T. Wijekoon, C. Klumpner, P. Zanchetta, and P. W. Wheeler, "Implementation of a hybrid AC–AC direct power converter with unity voltage transfer," *IEEE Trans. Power Electron.*, vol. 23, no. 4, pp. 1918–1926, Jul. 2008.

[14]   J. Itoh and K. Fujita, "Novel unity power factor circuits using zero-vector control for single-phase input systems," *IEEE Trans. Power Electron.*, vol. 15, no. 1, pp. 36–43, Jan. 2000.

[15]   J.-i. Itoh, I. Sato, A. Odaka, H. Ohguchi, H. Kodachi, and N. Eguchi, "A novel approach to practical matrix converter motor drive system with reverse blocking IGBT," *IEEE Trans. Power Electron.*, vol. 20, no. 6, pp. 1356–1363, Nov. 2005.

[16]   K. Kato and J.-i. Itoh, "Control method for a three-port interface converter using an indirect matrix converter with an active snubber circuit," in *Proc. 13th Power Electron. Motion Control Conf.*, Poznan, Sep. 2008, pp. 581–588.

[17]   J.-i. Itoh, S. Ikuya, O. Hideki, S. Kazuhisa, O. Akihiro, and E. Naoya, "A control method for the matrix converter based on virtual AC/DC/AC conversion using carrier comparison method," *IEEJ Trans. Ind. Appl.*,vol. 152, no. 3, pp. 65–73, Jun. 2005.

[18]   J.-i Itoh, T. Iida, and A. Odaka, "Realization of high efficiency AC link converter system based on AC/AC direct conversion techniques with RBIGBT," in *Proc. 32nd Ann. Conf. IEEE Ind. Electron.*, Paris, Nov. 2006, pp. 1703–1708.

[19]   S. Round, F. Schafmeister, M. Heldwein, E. Pereira, L. Serpa, and J. W. Kolar, "Comparison of performance and realization effort of a very sparse matrix converter to a voltage dc link pwm inverter with active front end," *IEEJ Trans. Inst. Electr. Eng. Jpn.*, vol. 126-D, no. 5, pp. 578–588, May 2006.